JBC RESEARCH ARTICLE

Development of a universal antibiotic resistance screening reporter for improving efficiency of cytosine and adenine base editing

Received for publication, December 23, 2021, and in revised form, May 26, 2022 Published, Papers in Press, June 6, 2022,
https://doi.org/10.1016/j.jbc.2022.102103

Lixia Ma[1,2,‡], **Jiani Xing**[1,‡], **Qian Li**[1], **Zhiying Zhang**[1,*], **and Kun Xu**[1,*]

From the [1]*Key Laboratory of Animal Genetics, Breeding and Reproduction of Shaanxi Province, College of Animal Science and Technology, Northwest A&F University, Yangling, Shaanxi, China;* [2]*Central Laboratory, Changzhi Medical College, Changzhi, Shanxi, China*

Edited by Patrick Sung

Base editing has emerged as a revolutionary technology for single nucleotide modifications. The cytosine and adenine base editors (CBEs and ABEs) have demonstrated great potential in clinical and fundamental research. However, screening and isolating target-edited cells remains challenging. In the current study, we developed a universal *Adenine and Cytosine Base-Editing Antibiotic Resistance Screening Reporter* (ACBE-ARSR) for improving the editing efficiency. To develop the reporter, the CBE-ARSR was first constructed and shown to be capable of enriching cells for those that had undergone CBE editing activity. Then, the ACBE-ARSR was constructed and was further validated in the editing assays by four different CBEs and two versions of ABE at several different genomic loci. Our results demonstrated that ACBE-ARSR, compared to the reporter of transfection (RoT) screening strategy, improved the editing efficiency of CBE and ABE by 4.6- and 1.9-fold on average, respectively. We found the highest CBE and ABE editing efficiencies as enriched by ACBE-ARSR reached 90% and 88.7%. Moreover, we also demonstrated ACBE-ARSR could be employed for enhancing simultaneous multiplexed genome editing. In conclusion, both CBE and ABE activity can be improved significantly using our novel ACBE-ARSR screening strategy, which we believe will facilitate the development of base editors and their application in biomedical and fundamental research studies.

The CRISPR/Cas9-based genome editing methods, including gene knock-in, KO, and point mutation, as well as small or large insertion and deletion, have been widely applied in different cells and organisms with great efficiency and accuracy (1–3). Single-guide RNA (sgRNA) guides the Cas9 endonuclease to introduce DNA double-stranded breaks (DSBs) at the desired target sites (4–6), and the DSBs are repaired by cellular endogenous repair systems such as nonhomologous end joining (NHEJ) or homology-directed repair (HDR) (7, 8). NHEJ takes up the dominant role but often leads to gene disruptions due to the error-prone insertion or deletion (indels) in DNA sequences (9). HDR is considered as an accurate repair, but the spontaneous efficiency is extremely low and requires active cell division (10, 11).

The emergence of engineered base editor (BE) has made up for the shortcomings of the CRISPR/Cas9 technology. Compared with the inefficient CRISPR/Cas9-based HDR (12), much higher base-editing efficiency can be achieved by the base editing technology without DSB induction and exogenous template. To date, there are many types of BEs with different deaminases, targeting windows, editing efficiencies, and protospacer adjacent motif (PAM) specificities (13, 14). The cytosine base editor (CBE), which induces C to T mutation (or G-to-A on the complementary strand) (15), and the adenine base editor (ABE), which mediates the change of A-to-G (or T-to-C on the complementary strand) have been well established (16). Since its development, the BE technology has been rapidly and widely used in various organisms (12, 17–19). These BEs play important roles in generating animal models (20) and correcting pathogenic mutations in somatic cells (21).

Although the efficiency of BE is much higher than CRISPR/Cas9-mediated HDR-based point mutation, it is still time consuming and laborious to isolate the base-edited cells from the cell population, especially for the target sites with low editing efficiency or the host cells hard to transfect such as induced pluripotent stem cells. The reporter of transfection (RoT) strategies by cotransfecting a plasmid containing fluorescent protein or antibiotic-resistant genes or fusing the marker genes to Cas9 have been used to select the transfection-positive or Cas9 expression-positive cells (22–24). However, the RoT strategies lack the capability to directly measure the BE activity (25). Consequently, real-time methods to identify and to enrich *in situ* the base-editing activity remain to be established.

In this work, we developed a novel universal screening reporter for both CBE and ABE, named *Adenine and Cytosine Base-Editing Antibiotic Resistance Screening Reporter* (ACBE-ARSR). The ACBE-ARSR was demonstrated versatile for improving the editing efficiency by different CBE and ABE. We believe that the ACBE-ARSR will facilitate the generation of base-edited cell models in biomedical and translational studies.

‡ These authors contributed equally to this work.
* For correspondence: Kun Xu, xukunas@nwafu.edu.cn; Zhiying Zhang, zhangzhy@nwafu.edu.cn.

© 2022 THE AUTHORS. Published by Elsevier Inc on behalf of American Society for Biochemistry and Molecular Biology. This is an open access article under the CC BY-NC-ND license (http://creativecommons.org/licenses/by-nc-nd/4.0/).

Results

Development of the CBE-ARSR for cytosine base editing

To develop a strategy for enriching and screening the base-edited cells based on the recovery of puromycin-resistance function, we firstly conducted site-directed mutagenesis focused on three residues of *PuroR* gene of pPuroR-T2A-eGFP vector (the initiation codon ATG-ACG, third codon GAG-GAA, and fourth codon TAC-TGC). The mutation vector, pmPuroR-T2A-eGFP (m means mutation), was predicted to cause a frame shift of *PuroR* gene, producing an altered and nonfunctional protein (Fig. 1*A*). To validate function of the two vectors, pmPuroR-T2A-eGFP and pPuroR-T2A-eGFP were transiently transfected into human embryonic kidney 293T (HEK293T) cells, respectively. As expected, untransfected HEK293T cells and cells transfected with pmPuroR-T2A-eGFP did not survive after 72 h of selection with puromycin, while cells transfected with pPuroR-T2A-eGFP could resist puromycin selection (Fig. 1*B*).

Inspired by this observation, we constructed a novel reporter construct, named CBE-ARSR. The CBE-ARSR reporter vector contains three components: a universal sgRNA expression cassette driven by the U6 promoter, a *PuroR* gene (the start codon ATG had been mutated) containing the universal sgRNA target sequence, and an ATG-removed *eGFP* cassette fused in frame with the upstream *PuroR* gene by a T2A self-cleavage peptide. For further application, we created a necessary NGG PAM for SpCas9 by introducing a mutation from threonine 7 (T7) to arginine (R) of the *PuroR* gene (Fig. 1*C*). Two versions of CBE-ARSR have been designed, one with a single ACG (CBE-ARSR-1 × ACG) and the other with two ACGs (CBE-ARSR-2 × ACG). With the guidance of the universal sgRNA, CBE can convert the 'ACG' to 'ATG', leading to expression of a functional PuroR and eGFP (Fig. 1*D*). We speculated that the C-to-T conversion of two ACG within the editing window (the two target Cs are located at position 4 and 7, respectively) would reflect the base-editing activity within a cell more sensitively than only one ACG (the target C is located at position 7 of editing window).

To tune the system, we first transfected the HEK293T cells with CBE-ARSR-1 × ACG or CBE-ARSR-2 × ACG and the untransfected HEK293T cells as the control group. The transfected cells were then subjected to puromycin treatment for 24 h, 48 h, 72 h, and 96 h, respectively, starting at 48 h post-transfection. In principle, the initiation codon of *PuroR* in CBE-ARSR reporter was not repaired, cells transfected with CBE-ARSR alone did not express *eGFP*, which was in frame with *PuroR*. Unexpectedly, although the cells transfected with CBE-ARSR-1 × ACG and CBE-ARSR-2 × ACG failed to resist puromycin selection, green fluorescence was observed at 48 h post-transfection (Fig. 1*E*). It is clear from the aforementioned results that the *PuroR* gene without an ATG is nonfunctional under the control of the cytomegalovirus (CMV) promoter but the *eGFP* expression cassette is functional. We suspected that it's caused by the transcription initiated by the ATGs internal to the *PuoR* gene sequence, which are in frame with T2A-eGFP. The relative cell viability detected by Cell Counting Kit-8 (CCK8) assay revealed that cells transfected with two versions of reporter, similar to the nontransfection control, were sensitive to the puromycin selection, as the relative cell viability dramatically decreased as the puromycin treatment time increased (Fig. 1*F*). After taking into consideration of puromycin selection time and cells viability, 72 h was used as the selection time of puromycin treatment in all of the following experiments unless noted otherwise. Next, CBE-ARSR-1 × ACG was transfected alone or cotransfected with YE1-BE3-FNLS into HEK293T cells. Fluorescence microscopy examination (Fig. 1*G*) and CCK8 assay (Fig. 1*H*) revealed that generation of PuroR/eGFP double-positive cells when the reporter was edited by YE1-BE3-FNLS successfully.

Based on these results, we can conclude that under corresponding universal sgRNA guidance, YE1-BE3-FNLS would convert 'ACG' to 'ATG', resulting in a functional PuroR expression. Collectively, these results indicate that the CBE-ARSR can be used as a reporter for screening cells that had undergone CBE editing activity.

CBE-ARSR mediated improvement of cytosine base-editing efficiency

The results of fluorescence microscopy showed that two versions of CBE-ARSR reporter either repaired or not by CBE, expressed constitutive GFP. In order to explore the reason behind this phenomenon, we carefully checked the PuroR-T2A-(ΔATG)eGFP cassette. In addition to the start codon ATG that was mutated to ACG, we found two internal 'ATG' and the second frame-shift 'ATG' introduced for inactivating the *PuroR* gene transcription (Fig. 2*A*). We speculated that the ORF starting from two internal 'ATG' causes the continuous *eGFP* expression. To address this question, we constructed 1 × ACG-3 × Flag and 2 × ACG-3 × Flag reporter vectors by fusing 3 × Flag tag to the C terminus of the *PuroR* in CBE-ARSR-1 × ACG and CBE-ARSR-2 × ACG. Using puromycin selection and fluorescence microscopy, we confirmed that 1 × ACG-3 × Flag and 2 × ACG-3 × Flag reporter vectors expressed eGFP but not PuroR, suggesting the 3 × Flag tag fusion did not affect the function of the original vectors (Fig. 2*B*).

The Western blot (WB) analysis showed that when the 1 × ACG-3 × Flag and 2 × ACG-3 × Flag reporters were not edited by YE1-BE3-FNLS, two PuroR-3 × Flag variants (∼19 kDa and ∼16 kDa) were encoded by #3 and #4 'ATG', respectively. When the #1 'ATG' was restored by YE1-BE3-FNLS, an intact and functional PuroR-3 × Flag protein (∼35 kDa) was expressed (Fig. 2*C*). The WB result also confirmed our speculation mentioned previously that the eGFP continuously expression resulting from the presence of additional ORFs. PuroR-3 × Flag proteins (∼35 kDa) were quantified, and the result showed that PuroR-3 × Flag (∼35 kDa) in 1 × ACG-3 × Flag is significantly higher than that in 2 × ACG-3 × Flag (Fig. 2*D*).

The primary purpose for developing CBE-ARSR reporter system was primarily intended to screen cytosine base-edited cells, in turn enhance editing efficiency of the target locus.

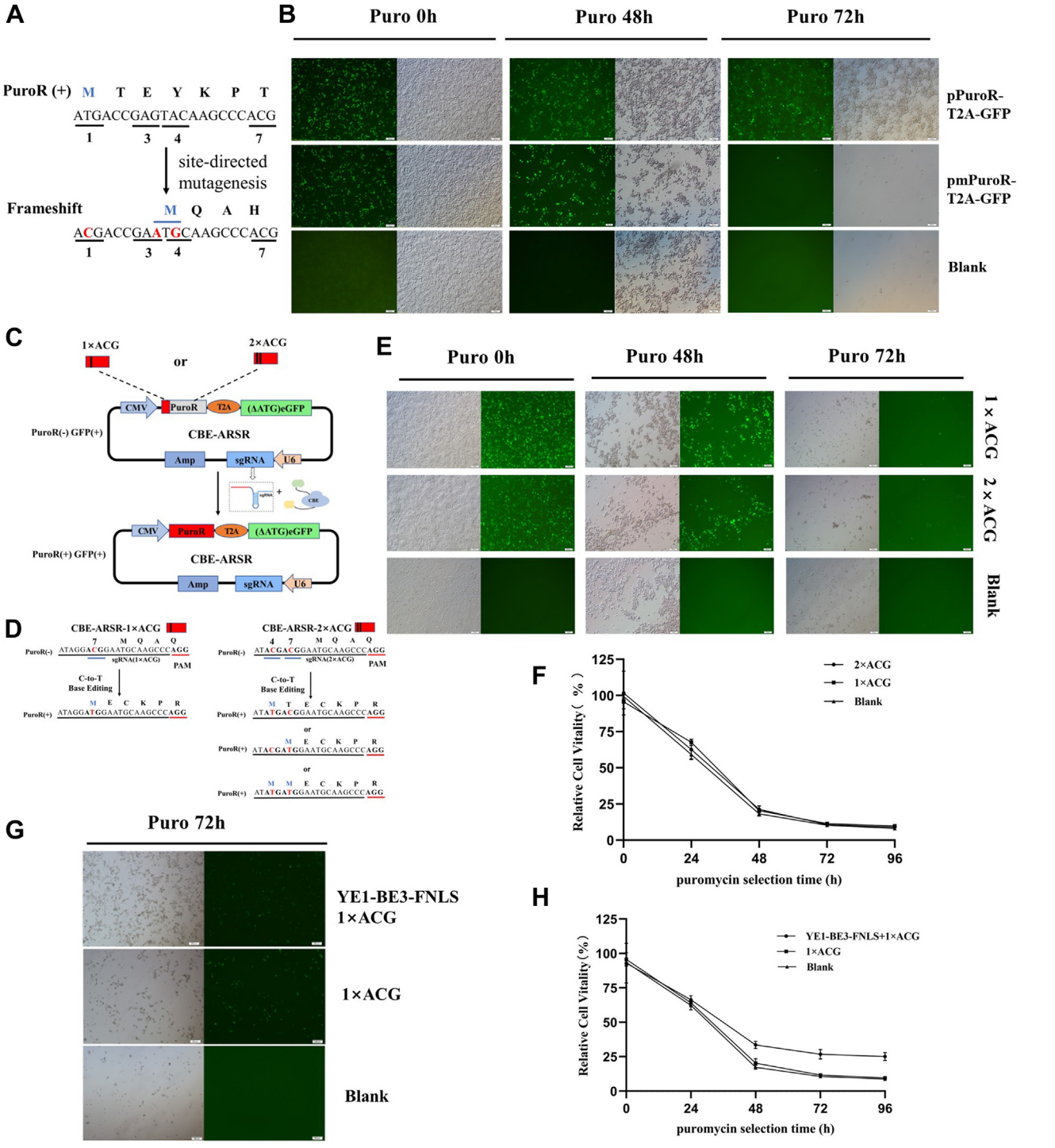

Figure 1. Design of the CBE-ARSR and preliminary functional analysis. *A*, schematic representation of site-directed mutagenesis of *PuroR* gene. Bases in *red* indicate mutated bases. *B*, mutations in the *PuroR* gene result in a complete loss of PuroR function. HEK293T cells transfected with pPuroR-T2A-eGFP or pmPuroR-T2A-eGFP were visualized by fluorescence microscopy at the indicated time points (0 h, 48 h, and 72 h after puromycin screening, respectively). HEK293T cells without any treatment were used as the blank control (Blank). The scale bar represents 100 μm. *C*, diagram of the CBE-ARSR system. The CBE-ARSR vector contains a CMV promoter-driven *PuroR* and (ΔATG)*eGFP* (the starting codon ATG of *PuroR* is replaced with ACG codon) and a U6 promoter-driven universal sgRNA expression cassette. The target sequence of the universal sgRNA is present in the 5′ end of the *PuroR* gene (containing the ACG codon) in the CBE-ARSR plasmid. Targeting CBE-ARSR with CBE will result in a C-to-T conversion, enabling restore the correct ORF of *PuroR* gene. *D*, two versions of CBE-ARSR plasmid, one with an ACG codon (CBE-ARSR-1 × ACG) and another with two ACG codons (CBE-ARSR-2 × ACG). The protospacer sequence (underlined *black*) for the universal sgRNA, CBE is guided by sgRNA to perform C-to-T conversion, resulting in ACG (underlined *blue*) becoming ATG and restoring PuroR expression. The PAM sequence was underlined in *red*, and the target 'C' were placed at positions 4 and 7 of base-editing window. Fluorescence microscopy (*E*) and CCK8 assay (*F*) analysis of HEK293T cells viability at the indicated time points after transfection with CBE-ARSR-1 × ACG or CBE-ARSR-2 × ACG. The scale bar represents 100 μm. Fluorescence microscopy (*G*) and CCK8 assay (*H*) analysis of HEK293T cells viability transfected with CBE-ARSR-1 × ACG and YE1-BE3-FNLS at the indicated time points. The scale bar represents 200 μm. ARSR, *Antibiotic Resistance Screening* Reporter; CBE, cytosine BE; CCK8, cell counting Kit-8; CMV, cytomegalovirus; sgRNA, single-guide RNA.

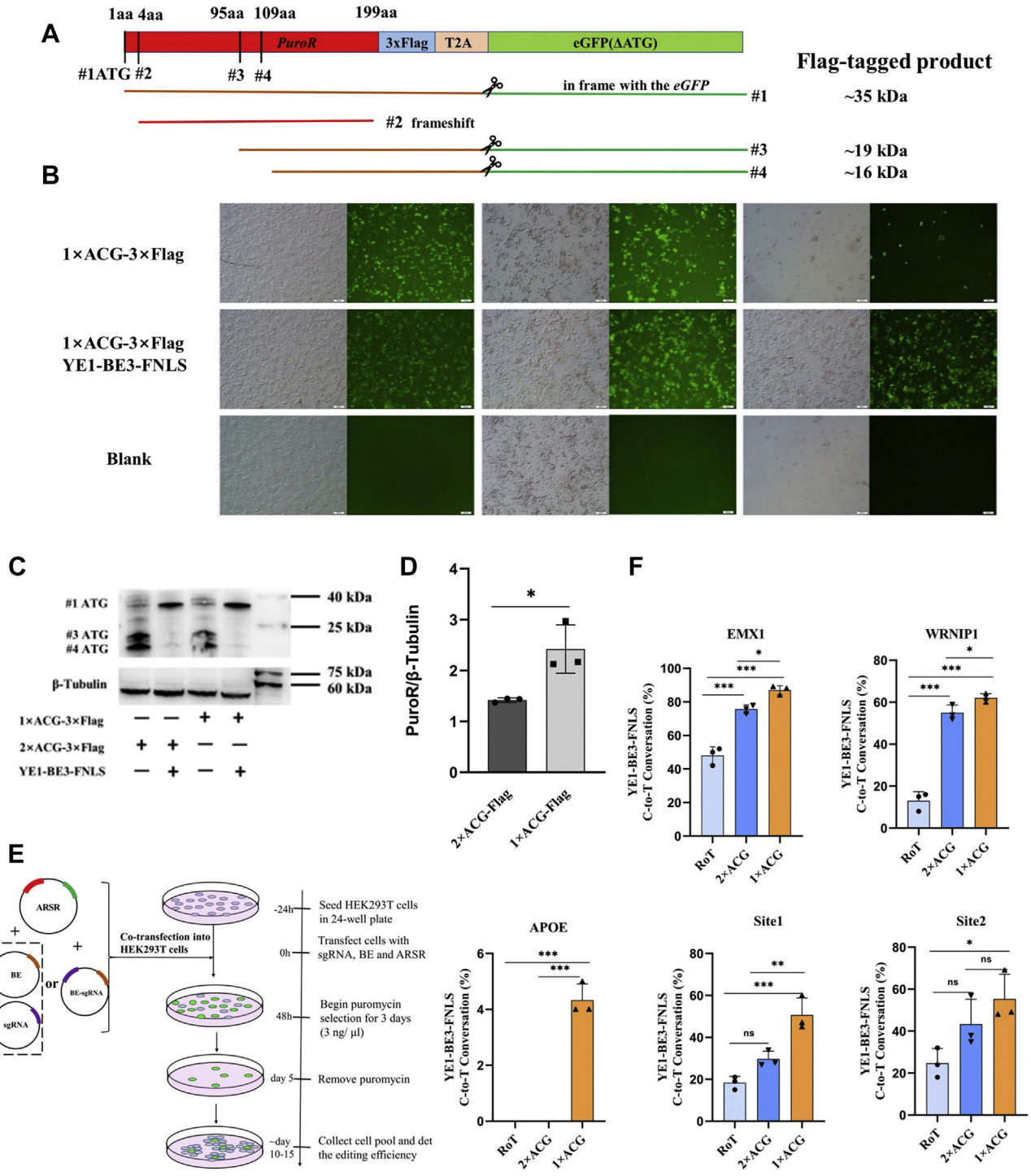

Figure 2. Tagged CBE-ARSR functional analysis and enhanced cytosine base editing. *A*, the structure schematics of four 'ATG' in *PuroR* gene. #1 'ATG' encode complete and functional PuroR protein, #2 'ATG' led to a frameshift mutation, #3 and #4 'ATG' encode two truncated and nonfunctional proteins. The expression of *eGFP* gene in frame with *PuroR* gene in the three 'ATG' (#1, #3, and #4). *B*, puromycin selection and cell morphology examination confirmed that the 3 × Flag tag fusion did not affect the function of the original reporter. The scale bar represents 100 μm. *C*, Western blot analysis of PuroR-3 × Flag expression in 1 × ACG-3 × Flag or 2 × ACG-3 × Flag vector before and after base editing by YE1-BE3-FNLS. *D*, relative expression of PuroR-3 × Flag between 1 × ACG-3 × Flag and 2 × ACG-3 × Flag, which were edited by YE1-BE3-FNLS. *E*, schematic for enrichment of cytosine base-edited cells using CBE-ARSR. *F*, comparison of the C to T conversion efficiency at five different gene loci in HEK293T cells enriched using RoT, CBE-ARSR-1 × ACG, and CBE-ARSR-2 × ACG strategies, respectively. *$p < 0.05$, **$p < 0.01$, ***$p < 0.001$, n = 3. ARSR, *Antibiotic Resistance Screening* Reporter; CBE, cytosine BE.

In order to compare the editing efficiency enriched by CBE-ARSR-1 × ACG and CBE-ARSR-2 × ACG, we constructed five sgRNA vectors targeting five genomic loci (EMX1, WRNIP1, APOE, Site1, and Site2). The information of Site1 and Site2 from referencess (26, 27). Cotransfected HEK293T cells with YE1-BE3-FNLS, sgRNA vector, and CBE-ARSR-1 × ACG or CBE-ARSR-2 × ACG. In addition, we wanted to compare the editing efficiency of CBE-ARSR with

conventional RoT strategies. As a RoT control group, cotransfected HEK293T cells with YE1-BE3-FNLS, sgRNA vector, and pPuroR-T2A-eGFP. Forty-eight hours after transfection, the cells were screened with 3 ng/μl puromycin for 3 days. Genomic DNA was extracted from the PuroR-positive cells and the targeted genomic sites were subject to Sanger sequencing after PCR amplification (Fig. 2*E*). C-to-T editing efficiencies of the target loci were analyzed by Sanger sequencing and BEAT programs https://hanlab.cc/beat/.

Compared to RoT strategy, both CBE-ARSR-1 × ACG and CBE-ARSR-2 × ACG could increase base-editing efficiency at all five gene loci. The average base-editing efficiency of PuroR-positive cells enriched using CBE-ARSR-1 × ACG system was about 2.98-fold of that in RoT strategies, suggesting that the CBE-ARSR-1 × ACG reporter system can significantly increase the base-editing efficiency compared to RoT enrichment strategy. Particularly for APOE, a difficult to edit locus, both RoT and CBE-ARSR-2 × ACG did not enrich edited positive cells, while CBE-ARSR-1 × ACG achieved a 4.6% base-editing efficiency (Fig. 2*F*). Accordingly, it is reasonable to suggest that the difference in enrichment of base-editing efficiency between two reporters is due to different PuroR expression levels after CBE editing.

Thus, the CBE-ARSR reporter system is more efficient and feasible to screen base-edited positive cell populations than conventional RoT strategies, particularly for some loci that were recalcitrant to editing.

Engineering a universal ACBE-ARSR for both ABE and CBE

Some of the fluorescence-based reporters were previously designed based on the assumption that a stop codon TAG/TGA can be converted to TGG by ABE, so that a fluorescent gene downstream can be expressed and used for evaluating the ABE activity (26). To develop a universal surrogate reporter that can be used to simultaneously enrich the cells edited by either ABE or CBE, we constructed a new reporter vector ACBE-ARSR on the basis of CBE-ARSR-1 × ACG reporter construct for evaluating both adenosine base editing and cytosine base editing (Fig. 3*A*). ABE can convert A-to-G, thus allowing the conversion of ATA codon to other codons (such as ATG, GTA, and GTG codons). Only the second 'A' of ATA was converted to 'G', making the ACBE-ARSR vector express a functional PuroR protein. Considering that the base-editing window for most ABEs is positions 4 to 7, we put the second 'A' of ATA on position five, then ATA has a greater chance of being converted to ATG. In principle, either CBE or ABE can create an ATG start codon, activating *PuroR* expression in ACBE-ARSR (Fig. 3*B*).

To further determine whether ACBE-ARSR can restore puromycin resistance protein expression following CBE or ABE editing, we constructed ACBE-ARSR-3 × Flag by fusing a 3 × Flag tag to *PuroR* C terminus as we did previously. Then, ACBE-ARSR-3 × Flag was cotransfected with YE1-BE3-FNLS or ABE7.10 into HEK293T cells. The WB result showed two 3 × Flag-tagged protein (∼19 kDa and ∼16 kDa) were translated from two internal 'ATG' of the ACBE-ARSR reporter, as in CBE-ARSR. The full-length PuroR-3 × Flag (∼35 kDa) was translated when the initiation codon ATG of ACBE-ARSR was repaired by YE1-BE3-FNLS or ABE7.10 targeting (Fig. 3*C*). Further analysis showed the expression of full-length PuroR-3 × Flag was not significantly different among the ACBE-ARSR repaired with ABE7.10 or YE1-BE3-FNLS (Fig. 3*D*).

Since the first version of CBE was published, numerous variants have been developed recently. Among them, BE3 with a standard editing window (positions 4–8) is the most widely used CBE developed by David Liu lab (15). In order to reduce unwanted editing byproducts, on the basis of BE3, BE4max was developed with higher editing efficiency. YE1-BE3-FNLS is a CBE variant with narrowed base-editing window (positions 5–7) displaying a comparable or higher on-target editing efficiency compared with BE4max (28). As a variant, hA3A-BE3 exhibits significantly higher base editing frequencies than BE3, and its editing window (positions 2–13) is wider than BE3 (29).

To further determine whether ACBE-ARSR reporter can be restored by different versions of CBE, four versions of CBE described previously were cotransfected into HEK293T cells separately with ACBE-ARSR. A fluorescence microscopy examination showed that all of these CBE could restore PuroR expression of the ACBE-ARSR; however, their relative editing activities are different among four types of CBE (Fig. 3*E*). Relative cell viability was determined using CCK8 assay, and the results showed that BE4max had the highest editing activity, followed by YE1-BE3-FNLS, hA3A-BE3, and BE3 that is consistent with the result reported by Zuo *et al* (28) (Fig. 3*F*).

ABE7.10 is one of the most efficient and widely used versions of ABE, and its editing window is typically found at protospacer positions 4 to 7(16). Zhou *et al*. developed ABE7.10F148A by introducing an F148A mutation into both TadA and TadA* of ABE7.10. Although ABE7.10F148A has a narrower window, it maintains a high level of editing efficiency compared to ABE7.10 (30). Then, HEK293T cells were cotransfected with ABE7.10 or ABE7.10F148A vectors along with the ACBE-ARSR. Notably, both of ABE7.10 and ABE7.10F148A could restore PuroR expression of the ACBE-ARSR reporter (Fig. 3*G*) and ABE7.10 showed higher base-editing activity than ABE7.10F148A (Fig. 3*H*).

To further confirm ACBE-ARSR can be used to improve the editing efficiency of various BEs, we compared the base-editing efficiency of BE4max and hA3A-BE3 at EMX1 locus. HEK293T cells were transfected with ACBE-ARSR, sgEMX1, and BE4max or hA3A-BE3, respectively. Then next-generation sequencing was performed on PCR amplicons of the EMX1 locus, and the results confirmed BE4max had a significant higher editing efficacy than hA3A-BE3 (Fig. 3*I*, top panel). Similarly, ABE7.10 exhibited higher editing activity than ABE7.10F148A at Site1 and Site3 loci (Fig. 3*I*, *middle* and *bottom panels*). The deep sequencing analyses were consistent with those shown in Figure 3, *F* and *H*.

Consequently, the ACBE-ARSR reporter can be employed to evaluate relative editing efficiency of different versions of CBE or ABE and screen base-edited positive cell populations.

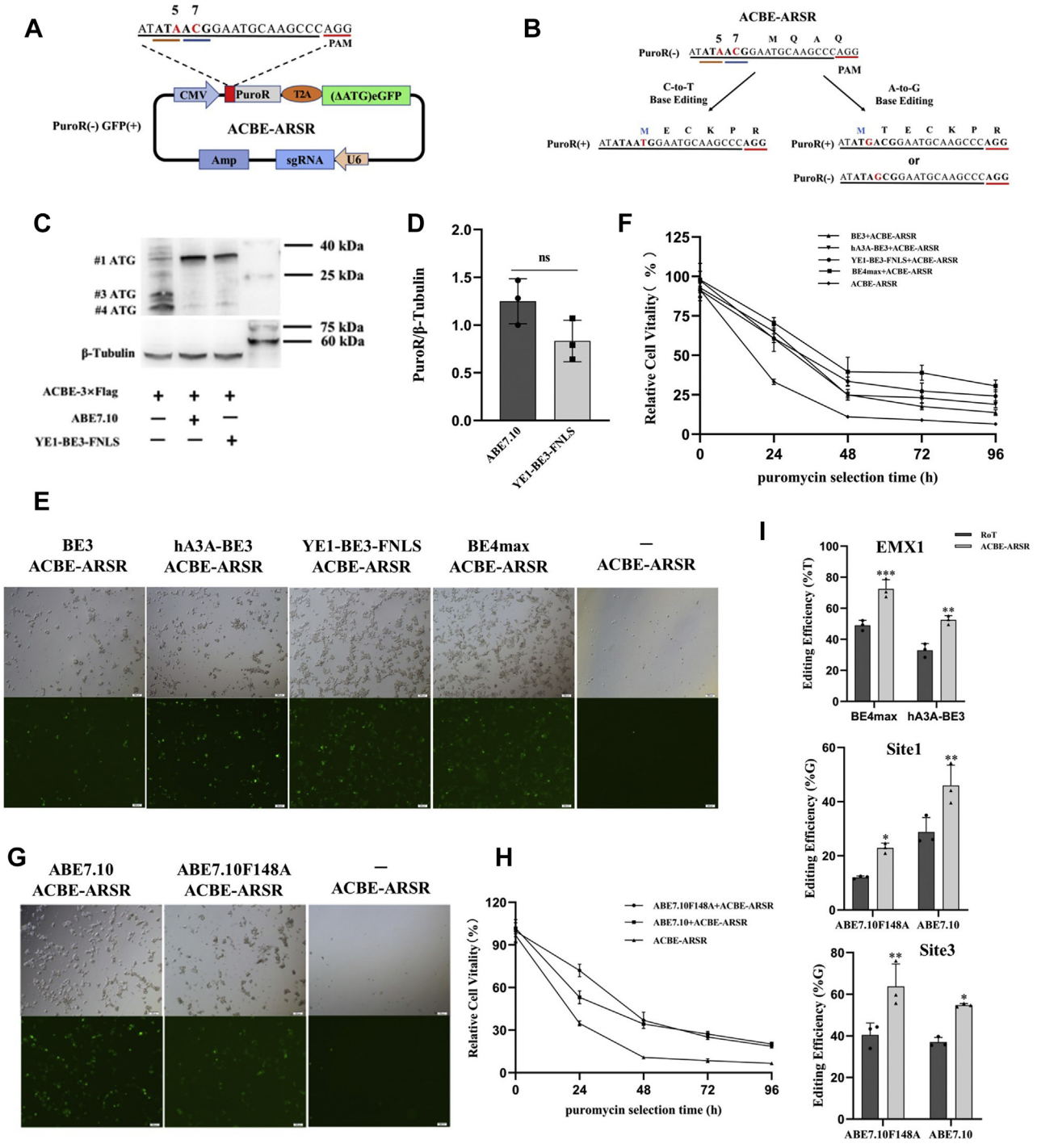

Figure 3. Design of the ACBE-ARSR and the functional analysis. *A*, a schematic diagram of the ACBE-ARSR reporter construct. A and C nucleotides are shown in *red* at the fifth and seventh positions of the editing window, respectively, indicating the target sites for ABE and CBE. The PAM sequence was underlined in *red*. *B*, sgRNA-CBE targets the 'ACG' codon (underlined *blue*) causing the conversion of 'ACG' to 'ATG' and initiating *PuroR* gene expression. sgRNA-ABE targets the 'ATA' codon (underlined *brown*) resulting in 'ATA' conversion to 'ATG' and initiating *PuroR* gene expression. *C*, analysis of the expression of PuroR-3 × Flag by Western Blot in HEK293T cells transfected with ACBE-ARSR-3 × Flag alone or cotransfected ACBE-ARSR-3 × Flag and different base editors (YE1-BE3-FNLS and ABE7.10). *D*, a comparison of full-length PuroR-3 × Flag expression in ACBE-ARSR-3 × Flag vector edited by YE1-BE3-FNLS or ABE7.10. *E*, ACBE-ARSR reporter can be restored by different CBE variants (BE3, hA3A-BE3, YE1-BE3-FNLS, and BE4max). HEK293T cells were transiently transfected with ACBE-ARSR and one of four version CBE. Cell viability was assessed by fluorescence microscopy after puromycin selection for 72 h. The scale bar represents 200 μm. *F*, relative cell viability in each group after puromycin selection was determined by CCK-8 assay, the grouping was the same as (*E*). *G*, ACBE-ARSR reporter can be restored by two ABE variants (ABE7.10 and ABE7.10F148A). The scale bar represents 200 μm. *H*, relative cell viability in each group after puromycin selection was determined by CCK-8 assay, the grouping was the same as (*G*). *I*, deep sequencing quantification of C-to-T and A-to-G editing efficiency on PCR amplicons generated from pooled genomic DNA. $^{*}p < 0.05$, $^{**}p < 0.01$, $^{***}p < 0.001$, n = 3. ABE, adenine BE; ACBE-ARSR, *Adenine and Cytosine Base-Editing Antibiotic Resistance Screening* Reporter; BE, base editor; CBE, cytosine BE; CCK8, Counting Kit-8; sgRNA, single-guide RNA.

ACBE-ARSR meditated enhanced base-editing by different ABE and CBE

Based on the phenomenon of 'cotargeting with selection' in genome-editing experiments, we envisioned that successful editing of the ACBE-ARSR surrogate reporter could allow us to enrich cells in which endogenous target loci had been edited by CBE or ABE.

To utilize ACBE-ARSR for the enrichment of cells that have been edited by CBE at five target loci (EMX1, WRNIP1, APOE, Site1, and Site2) respectively, we cotransfected sgRNA vector with ACBE-ARSR and different versions of CBE into HEK293T cells. To utilize ACBE-ARSR for the enrichment of cells that have been edited by ABE at three target loci, respectively (Site1, Site2, Site3), we cotransfected sgRNA vector, ACBE-ARSR and one version of ABE into HEK293T cells. Cotransfected HEK293T cells with pPuroR-T2A-eGFP, BE, and sgRNA vector as RoT control group. Forty-eight hours post-transfection, the base-edited cells were enriched with puromycin (3 ng/ul) for 3 days. Then, these puromycin-resistant cell populations were analyzed for base editing of the genomic sites by Sanger sequencing and the BEAT software (https://hanlab.cc/beat/).

In conclusion, regardless of the CBE variant used, statistical analysis confirmed that ACBE-ARSR enriched the C-to-T base editing efficiency significantly higher than that enriched by RoT at all of the five genomic sites (Fig. 4*A*). The editing efficiencies at target loci were summarized in Table 1; we found the highest CBE editing efficiency enriched by ACBE-ARSR reached up excitingly 90%. The editing efficiency of CBE enriched by ACBE-ARSR system was, on average, 4.6-fold than those from RoT strategy. The APOE locus is strongly associated with Alzheimer's disease, and analysis of PCR amplification products of the locus revealed that cells enriched using RoT-based approach had a very low editing efficiency. Surprisingly, ACBE-ARSR system achieved efficient editing in APOE locus, which was edited by BE4max, it was 6.4-fold in editing efficiency that of RoT method (Fig. 4*B* and Table 1).

Similarly, we observed ACBE-ARSR enrichment system could be enriched effectively by ABE7.10 and ABE7.10F148A edited-positive cells at all tested sites than RoT enrichment strategies (Fig. 4, *C* and *D*). The highest ABE editing efficiency enriched by ACBE-ARSR reached up to an amazing 88.7%. On average, the efficiency of adenosine base editing at three target loci using the ACBE-ARSR system was 1.9-fold than that of the RoT strategy (Table 1).

In summary, ACBE-ARSR is a universal surrogate reporter for the enrichment of cell populations edited by CBE and ABE. Compared to conventional RoT approaches, ACBE-ARSR allows for statistically significantly higher frequency of base editing at target sites.

Enhanced multiplex base editing by ACBE-ARSR

We finally investigated whether the ACBE-ARSR could be used for multiplexed genome modification. First, sgEMX1-Site2 was constructed, which targets EMX1 and Site2 simultaneously, and sgEMX1-Site2-Site1, which targets EMX1, Site2, and Site1 simultaneously (Fig. 5*A*). The ACBE-ARSR reporter was then cotransfected into HEK293T cells with YE1-BE3-FNLS and sgEMX1-Site2 or with YE1-BE3-FNLS and sgEMX1-Site2-Site1 to achieve base editing of multiple loci, simultaneously. In parallel, we used RoT-based approach as control groups that HEK293T cells were cotransfected with pPuroR-T2A-eGFP, YE1-BE3-FNLS, and sgEMX1-Site2 or sgEMX1-Site2-Site1. After puromycin selection, puromycin resistance cells were harvested. Sanger sequencing of the multiple targeted genomic sites in puromycin-resistant cells isolated from ACBE-ARSR and RoT approaches revealed that ACBE-ARSR allowed for statistically significant higher frequency of base editing than RoT approaches. As shown in Figure 5*B*, simultaneous editing at two sites, the editing efficiency of YE1-BE3-FNLS-mediated C-to-T conversion enriched using ACBE-ARSR was 83.7 ± 7.1% for EMX1 and 52 ± 6.2% for Site2, whereas the editing efficiency enriched using RoT was 42.7 ± 3.5% for EMX1 and 25.7 ± 3.2% for Site2. As shown in Figure 5*C*, for the ACBE-ARSR enrichment system, the C-to-T conversion efficiency were 78.3 ± 5%, 59.7 ± 4.5%, and 67.7 ± 5.1% for EMX1, Site1, and Site2 loci, respectively, that is also significantly higher than base-editing efficiency enriched by RoT.

Discussion

Compared with CRISPR/Cas9-based HDR-mediated point mutations, BEs are more efficient in correcting point mutations and produce fewer by-product indels (12). According to the ClinVar database, about 60% of genetic diseases caused by single-base mutations can be corrected by CBE and ABE (31, 32). Despite the advantages of BEs, it is still a time consuming and laborious task to isolate and obtain desired edited cells from the large cell population, especially for the target loci with low editing efficiency. Just as we summarized previously, gene editing efficiency is usually limited by transfection efficiency, nuclease activity, and DNA repair efficiency, and the selection and enrichment of gene-edited positive cells is always necessary in many biological studies (24).

Recently, several fluorescence-based reporters have been developed to report CBE or ABE activities (26, 27, 33–38). The codon CAC at the 66th position of BFP, when modified to 'TAC' or 'TAT' by CBE, can result in the amino acid change from histidine to tyrosine, making the fluorescence shift from BFP to GFP. Accordingly, two research teams developed transient reporters BE-FLARE and TREE for enriching cells edited by CBE (27, 36). Moreover, Martin *et al*. established a panel of *eGFP* reporters for CBEs based on the findings that three codons that have a T-to-C mutation ablates GFP fluorescence (37). The reporters for detecting and enriching ABEs edited cells were established by mediating A-to-G conversion in the TGA stop codon located in GFP frame or upstream of an ATG-removed *GFP* gene to evoke GFP expression, such as XMAS-TREE and BEON (26, 34, 35). It should also be noted that all of the reporters mentioned previously were designed for either CBE or ABE but not both.

Although the fluorescence-based screening strategy is intuitively, time-saving, and convenient, its application is

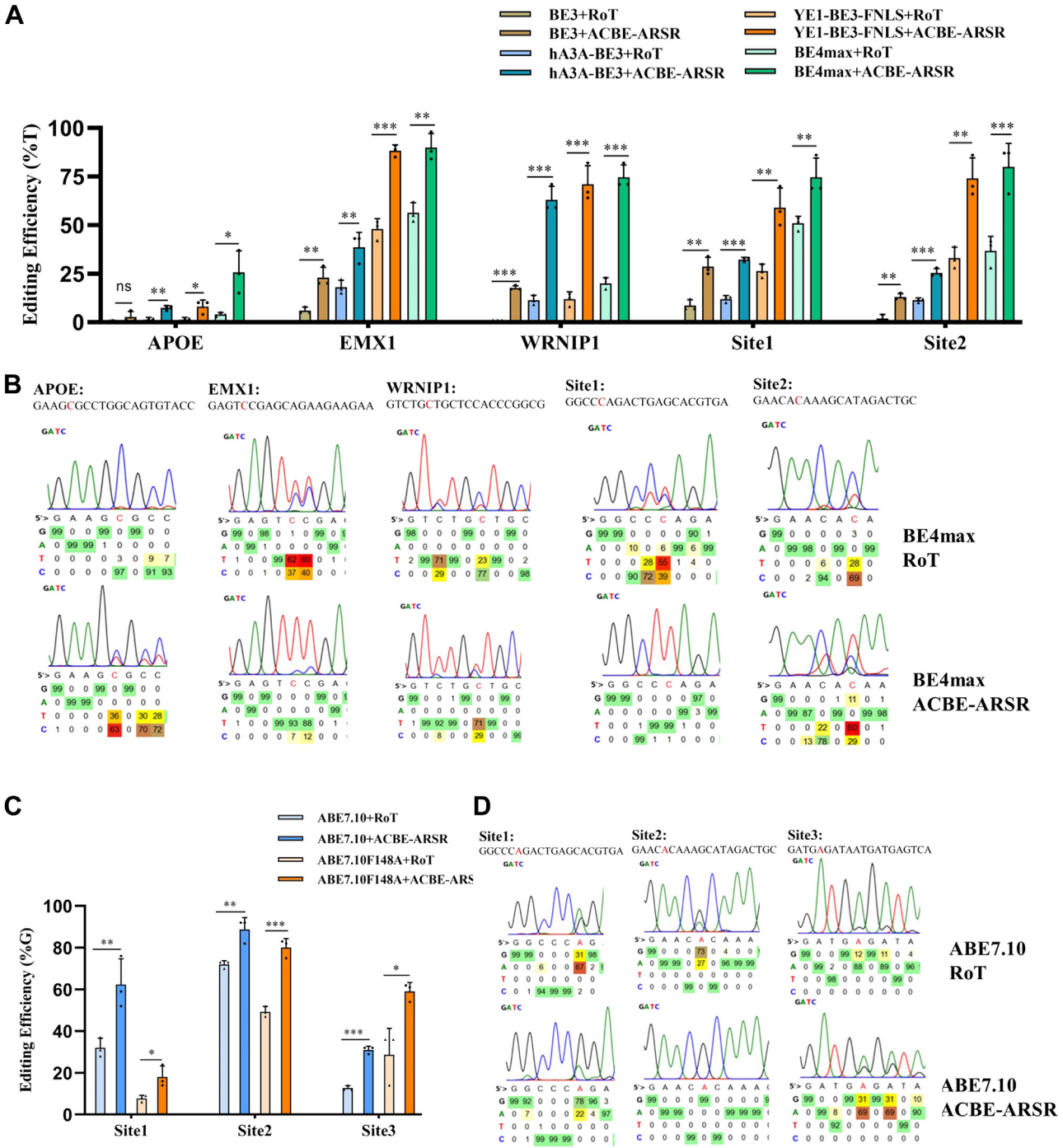

Figure 4. ACBE-ARSR improves the base-editing efficiency of different CBE and ABE. *A*, qualification of base-editing efficiency at five genomic loci in HEK293T cells enriched using ACBE-ARSR or RoT-based enrichment strategies. Five target sites were edited with four versions of CBE. *B*, representative chromatographs of Sanger sequencing results of the five target sites. The target 'C' in editing windows is labeled with *red*. BE4max + RoT, cells cotransfected with BE4max, the sgRNA plasmid, and pPuroR-T2A-eGFP; BE4max + ACBE-ARSR, cells cotransfected with BE4max, the sgRNA plasmid, and ACBE-ARSR. *C*, qualification of base-editing efficiency at three genomic loci in HEK293T cells enriched using ACBE-ARSR- or RoT-based enrichment strategies. Three target sites were edited with two versions of ABE. *D*, representative chromatographs of Sanger sequencing results of the three target sites. The target 'A' in editing windows is labeled with *red*. ABE7.10 + RoT, cells cotransfected with ABE7.10, the sgRNA plasmid, and pPuroR-T2A-eGFP; ABE7.10 + ACBE-ARSR, cells cotransfected with ABE7.10, the sgRNA plasmid, and ACBE-ARSR. *$p < 0.05$, **$p < 0.01$, ***$p < 0.001$, n = 3. ABE, adenine BE; ACBE-ARSR, *Adenine and Cytosine Base-Editing Antibiotic Resistance Screening* Reporter; BE, base editor; CBE, cytosine BE; RoT, reporter of transfection; sgRNA, single-guide RNA.

usually limited by the equipment flow cytometer. Besides, contamination and poor cell growth are also headache problems when cloning flow cytometry–sorted cells. On the other hand, antibiotic resistance-based screening strategy has also been usually used for screening gene-edited cells. Puromycin is a common antibiotic-resistance selection agent. Different puromycin selecting strategies have been developed, including the transfection-positive selection (39), the NHEJ-based (40), single strand annealing-based (41) and HDR-based (42) nuclease-active selections. Here, we developed the

Table 1
Base-editing efficiency by different CBE and ABE at different genomic loci

Targets / Editing efficiencies / Base editors		BE3	hA3A-BE3	YE1-BE3-FNLS	BE4max	Average improvement for CBE	ABE7.10	ABE7.10F148A	Average improvement for ABE
APOE	RoT	0.3 ± 0.6%	1.3 ± 1.2%	1.3 ± 1.1%	4 ± 1%				
	ACBE-ARSR	2.7 ± 2.8%	7.3 ± 1.1%	7.3 ± 1.1%	25.7 ± 11%				
	Fold	9	5.6	6.2	6.4	**6.8**			
EMX1	RoT	6 ± 1.7%	18 ± 3.6%	48 ± 5.3%	56.3 ± 5.1%				
	ACBE-ARSR	23 ± 5.2%	38.7 ± 7.5%	88.3 ± 3.1%	90 ± 7.2%				
	Fold	3.8	2.1	1.8	1.6	**2.3**			
WRNIP1	RoT	1%	11.3 ± 2.5%	12 ± 3.6%	20 ± 3%				
	ACBE-ARSR	17.7 ± 1.2%	63 ± 6.9%	71 ± 9.6%	74.7 ± 6.4%				
	Fold	17.7	5.6	5.9	3.7	**8.2**			
Site1	RoT	8.7 ± 2.9%	12 ± 1.7%	26.3 ± 3.5%	51 ± 3.6%		32 ± 4.6%	7.7 ± 1.5%	
	ACBE-ARSR	28.7 ± 4.7%	32.3 ± 1.2%	59 ± 10.1%	74.7 ± 9.8%		62.3 ± 12.3%	18 ± 5.2%	
	Fold	3.3	2.7	2.2	1.5	**2.4**	1.9	2.3	**2.1**
Site2	RoT	2 ± 2%	11.3 ± 1.1%	33 ± 5.6%	36.7 ± 7.6%		72 ± 1.7%	49.3 ± 2.5%	
	ACBE-ARSR	13 ± 1.7%	25.3 ± 2.3%	74 ± 10.6%	80 ± 12.1%		88.7 ± 5.7%	80 ± 4.3%	
	Fold	6.5	2.2	2.2	2.2	**3.3**	1.2	1.6	**1.4**
Site3	RoT						12.6 ± 1.1%	28 ± 12.7%	
	ACBE-ARSR						31 ± 1.7%	59 ± 4.3%	
	Fold						2.5	2.1	**2.3**
Average improvement in total						**4.6**			**1.9**

The bold value represents the average editing efficiency of the target locus which are edited by multiple types of BE.

ACBE-ARSR for the selection of BE editing positive cells, which will help to complete the jigsaw puzzle for the screening strategies of gene-edited positive cells. All of these surrogate reporter-based strategies apply transient puromycin selection (3–5 days) for the enrichment of gene-edited positive cells. What's more, stable puromycin selection (usually more than 1 week) has also been applied in the CRISPR/Cas9-based KO and transcriptional activation screening systems (43), as well as the BE-based screening systems (44, 45), for screening essential genes. All these applications suggest puromycin selection is a promising strategy for screening gene-edited cells in fundamental researches. Nevertheless, we must admit that the cytotoxicity and integration of the resistance gene cassette may be the major concerns for puromycin selection as well as other antibiotic resistance-based selecting strategies, which remain to be discussed.

Although we focused on enriching base-edited cells by puromycin-resistant selection in this work, it is easy to adapt our system to use fluorescent marker gene in order to enable enrichment of endogenous base editing by fluorescence-activated cell sorting. Indeed, a paralleled work by other researchers was published lately, reporting a Gene On system applied similar ACG > ATG strategy but just for improving CBE editing efficiency only by fluorescence-activated cell sorting sorting (34).

Notably, we conducted the experiments with three-plasmid transfection (the reporter, the Cas9-deaminase expression vector, and the separate sgRNA expression vector) for the convenience in the current study for comparing different BEs at different target sites, and in theory it does not seem to guarantee that base editing occurred at the desired genomic locus, since the reporter only labels cells in which the reporter and the Cas9-deaminase are present. However, it is usually assumed that cotransfection of mammalian cells with multiple plasmids could be achieved in a constant proportion (24, 46). And what's more, our results did demonstrate that the reporter improved the editing efficiency of the target genomic locus in the puromycin-selected cells. Nevertheless, further application of the reporter by combing the Cas9-deaminase and intent target sgRNA in a single plasmid (Fig. 2*E*) may guarantee the editing events at desired genomic locus.

Recently, a dual adenine and cytosine BE (A&C-BEmax) had been developed by fusing both deaminases to the Cas9 D10A (47). Simultaneous C-to-T and A-to-G conversions in a same target sequence could be achieved by A&C-BEmax, but the efficiency remains to be improved. We look forward to incorporation of our ACBE-ARSR into the A&C-BEmax in the subsequent investigation. We believe that ACBE-ARSR as a novel universal reporter will accelerate the development of new versions of BE and facilitate the application of CBE and ABE in biomedical and fundamental researches.

Experimental procedures

Construction of the RoT vector

Unless otherwise noted, PCR for molecular cloning were performed using Prime STAR Max (TAKARA). All restriction

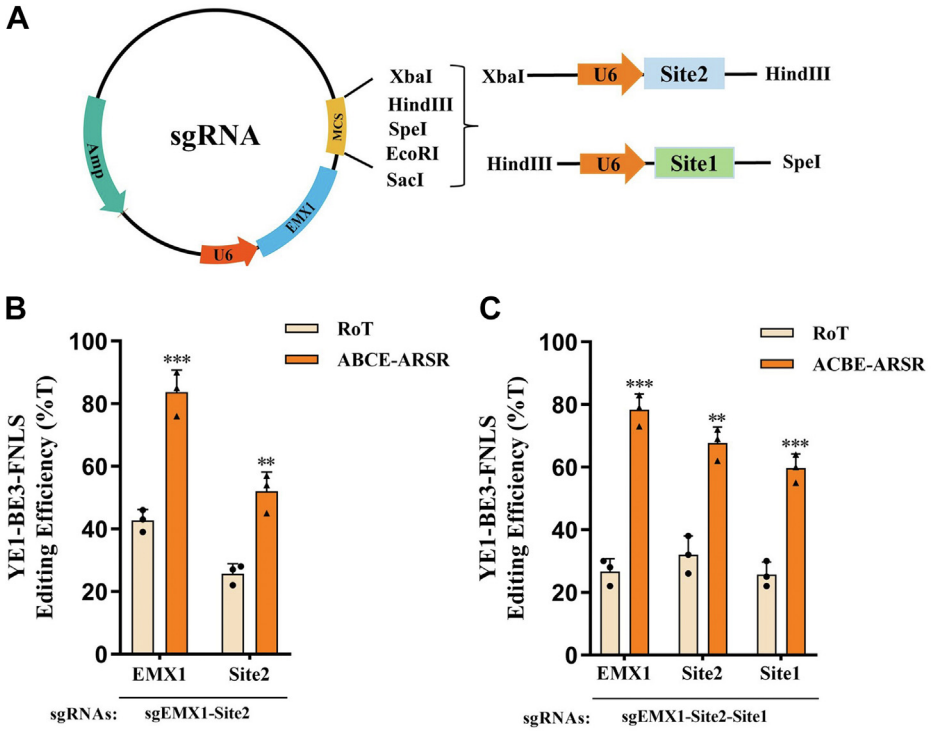

Figure 5. Enhanced simultaneous base editing of multiple sites using ACBE-ARSR. *A*, plasmid map of sgRNA vector that contains the multiple cloning site (MCS) allowing the insertion of multiple sgRNA expression cassettes that is driven by separate U6 promoters (*orange arrows*). *B*, analysis of base-editing efficiency at EMX1 and Site2 in HEK293T cells isolated using ACBE-ARSR or RoT-based enrichment strategies. *C*, analysis of base-editing efficiency at EMX1, Site2, and Site1 in HEK293T cells isolated using ACBE-ARSR or RoT-based enrichment strategies. *$p < 0.05$, **$p < 0.01$, ***$p < 0.001$, n = 3. ACBE-ARSR, *Adenine and Cytosine Base-Editing Antibiotic Resistance Screening* Reporter; RoT, reporter of transfection.

enzyme (TAKARA) digestions were performed according to the manufacturer's instructions. Ligation reactions were performed with T4 DNA Ligase (Servicebio) at 25 °C for 30 min according to the manufacturer's instruction. All PCR primers and oligonucleotides were synthesized by TSINGKE. All PCR products and intermediate plasmid products were sequenced confirmed *via* Sanger sequencing (TSINGKE).

The PuroR-T2A-eGFP expression cassette was amplified using primer CMV-F NcoI and GFP-R XbaI from plasmid pRS426-CMV-Puro-T2A-eGFP-polyA (42) and cloned into a NHEJ-based reporter plasmid in our lab (unpublished data) between NcoI and XbaI, generating pPuroR-T2A-eGFP. Primers were designed with desired base changes, then three mutated bases were introduced into *PuroR* gene by overlap PCR, and the resulting PCR products were inserted into the NcoI/AgeI sites of the vector pPuroR-T2A-eGFP giving rise to pmPuroR-T2A-eGFP vector.

Construction of the ARSR vectors

To construct universal screening reporter vectors, named CBE-ARSR-1 × ACG, CBE-ARSR-2 × ACG, and ABCE-ARSR, respectively, four main steps had to be completed. First, we constructed pmPuroR_NGG-T2A-eGFP vector by overlap-extension PCR introducing a point mutation to generate a PAM sequence (AGG) for spCas9. Second, modified the start codon of *PuroR* gene, generating p(ACG)PuroR_NGG-T2A-eGFP, p(ACGACG)PuroR_NGG-T2A-eGFP, and p(ATAACG)PuroR_NGG-T2A-eGFP. Third, the sgRNA sequences corresponding to the modified three *PuroR* sequences described previously were annealed into the pX330-U6-Chimeric_BB-CBh-hSpCas9 vector (#42230; Addgene) between BsaI, generating the sgRNA expression vectors p(ACG)sgRNA, p(ACGACG)sgRNA, and p (ATAACG) sgRNA, individually. Fourth, sgRNA expression cassettes were amplified from three sgRNA expression vectors and inserted into the corresponding vectors of the second step, respectively, generating the final vectors CBE-ARSR-1 × ACG, CBE-ARSR-2 × ACG, and ABCE-ARSR.

The 3 × Flag expression cassette was amplified using primer Flag-F and Flag-R from plasmid pX330-U6-Chimeric_BB-CBh-hSpCas9. The vectors 1 × ACG-3 × Flag, 2 × ACG-3 × Flag, and ABCE-ARSR-3 × Flag were constructed using homologous recombination kit (Vazyme, C112-01).

All primers used for constructing the transient transfection screening vector and the universal screening reporter vectors were listed in Table S1.

Construction of the sgRNA expression vectors

The Cas9 gene in pX330-U6-Chimeric_BB-CBh-hSpCas9 plasmid was replaced by a multiple cloning site sequence containing XbaI, HindIII, SpeI, EcoRI, and SacI enzyme sites using primer annealing method. We constructed six single-locus targeting plasmids and named them sgEMX1, sgWRNIP1, sgAPOE, sgSite1, sgSite2, and sgSite3. Double-loci–targeting plasmids were based on single-locus–targeting plasmids. In brief, fragment U6-Site1 was amplified from

sgSite1 using primer U6-F XbaI and scaffold-R HindIII and was inserted into the XbaI and HindIII sites of sgEMX1 plasmid, generating the vector sgEMX1-Site. The triple-loci–targeting plasmids were constructed by similar method. Primers and pairs of oligonucleotides corresponding to the target gene locus were listed in Table S2, and all sgRNA expressing vectors were confirmed by Sanger sequencing.

Cell culture and transfection

HEK293T cells were cultured in Dulbecco's modified Eagle's medium (Gibco) supplemented with 10% (v/v) fetal bovine serum (Gibco) and 1% 100 × penicillin–streptomycin (Gibco) in a 37 °C humidified atmosphere with 5% CO_2 incubation. Cells were plated in 24-well plates and were transfected with 600 ng plasmids (200 ng reporter, 200 ng sgRNA, and 200 ng BE) per well when cells confluency reached 70% to 80%. The transfection assays were conducted using Lipofectamine TM 3000 Reagent (Invitrogen) according to protocol strictly. Each group was performed three times for obtaining accurate results.

Puromycin selection

Forty-eight hours after transfection, 3 μg/ml puromycin (Invitrogen) was added to the culture medium and maintained for 72 h. During this period, the medium containing puromycin was changed every day. Then, the culture medium containing puromycin was removed, and the surviving cells were cultured sequentially until the cell confluency reached 90% for subsequent genome detection.

Determination of cell viability

Cell viability was monitored with CCK8 kit (CCK8, Dojindo) following the producer's suggestion. HEK293T cells were transfected with plasmids, and 48 h later, cells were digested, and 5×10^3 cells were seeded in a 96-well culture plates. Three replicate wells were set for each group. Once adherent, the cells were treated with puromycin (final concentration to 3 μg/ml) and the timepoint is defined as 0 h. Ten microliters CCK8 solution was added to each well at 0 h, 24 h, 48 h, 72 h, and 96 h, respectively, and incubated at 37 °C for 2 h, then the absorbance was measured at 450 nm with a microplate reader. In order to calculate relative cell viability, the untransfected group without puromycin treatment was used as the control. The following formula was used:

Relative cell viability (%) = $[(A_{\text{treatment}}\text{-}A_{\text{blank}})]/[A_{\text{control}}\text{-}A_{\text{blank}})] \times 100\%$.

Western blot analysis

Proteins were extracted 48 h after the transfection. Protein samples were resolved by electrophoresis in a 12% SDS-PAGE gel (Genscript; M00667) and were transferred to a polyvinylidene difluoride membrane in transfer buffer (Genscript; M00139) using a wet procedure at 300 mA for 1 h. Followed by blocking with 5% nonfat milk dissolved in TBST buffer (20 mM Tris-HCl, 150 mM NaCl, 0.05% (v/v) Tween 20) at room temperature (RT) for 1 h, the membranes were probed with anti–Flag-Tag mouse monoclonal antibody (1:2000, CWBIO, CW0287) and anti–β-tubulin mouse monoclonal antibody (1:2000, CWBIO, CW0098) overnight at 4 °C. The membrane was washed for 10 min with TBST buffer on an orbital shaker for three times and then incubated with goat antimouse secondary antibody (1:2000, CWBIO, CW0102S) at RT for 1 h and washed with TBST as described previously. Proteins were detected with ECL Western horseradish peroxidase substrate (Advansta) on a chemiluminescent gel imaging system (MicroChemi, DNR). EasySee Western Marker (Transgen; DM201-01) was used as molecular weight marker.

Quantification of base-editing efficiency

Genomic DNA was extracted from mixed pool of HEK293T cells using Genomic DNA Kit (TIANGEN). PCR was performed using 200 ng genomic DNA as the template in a 50 μl master mix containing of Prime STAR Max DNA Polymerase (TAKARA), 1 μM forward primer, and 1 μM reverse primer. PCR was performed using the following conditions: 95 °C for 3 min, followed by 35 cycles at 98 °C for 15 s, 58 °C for 15 s, and 72 °C for 10 s, followed by a final 5 min 72 °C extension. All PCR products were confirmed and purified by 1% agarose gel prior to Sanger sequencing. Base editing efficiencies were analyzed from Sanger sequencing traces using BEAT (48). Primers for amplification of the six target genes (EMX1, WRNIP1, APOE, Site1, Site2, and Site3) were listed in Table S3.

Next-generation sequencing of PCR amplicons

For deep sequencing, genomic DNA was used as the template. PCR was performed to amplify different target locus with primers with distinguishable barcodes. The PCR products were column purified using the PCR purification kit and amplicons were sequenced on an Illumina MiSeq by Sangon Biotech. The primers used for deep sequencing were listed in Table S4.

Statistical analysis

Experiments were independently replicated a minimum of three times, and data were displayed as mean ± SD. *t* Test was used to compare two groups of independent samples. Multiple comparisons were performed with one-way ANOVA and post hoc Tukey-test. *p* Value less than 0.05 was considered statistically significant.

Data availability

All data in this study are available within the article, supporting information, and/or from the corresponding author on reasonable request.

Supporting information—This article contains supporting information.

Acknowledgments—We thank professors Xingxu Huang, Xiaolong Wang, and Erwei Zuo for providing various versions of base editors.

This study was supported by grants from the National Natural Science Foundation of China (31702099) and the Key Project of Natural Science Basic Research Program of Shaanxi Province (2019JZ-07).

Author contributions—Z. Z., K. X., and L. M. conceptualization; Z. Z., K. X., and L. M. methodology; L. M., J. X., and Q. L. investigation; L. M. and J. X. writing–original draft; Z. Z. and K. X. writing–review & editing.

Conflict of interest—The authors declare that they have no conflicts of interest with the contents of this article.

Abbreviations—The abbreviations used are: ABE, adenine base editor; ACBE-ARSR, Adenine and Cytosine Base-Editing Antibiotic Resistance Screening Reporter; BE, base editor; CBE, cytosine base editor; CCK8, cell counting kit-8; CMV, cytomegalovirus; DSB, double-stranded break; HDR, homology-directed repair; NHEJ, nonhomologous end joining; PAM, protospacer adjacent motif; RoT, reporter of transfection; sgRNA, single-guide RNA; WB, Western blot.

References

1. Komor, A. C., Badran, A. H., and Liu, D. R. (2017) CRISPR-based technologies for the manipulation of eukaryotic genomes. *Cell* **169**, 559
2. Hartz, P., Gehl, M., Konig, L., Bernhardt, R., and Hannemann, F. (2021) Development and application of a highly efficient CRISPR-Cas9 system for genome engineering in Bacillus megaterium. *J. Biotechnol.* **329**, 170–179
3. Wright, A. V., Nunez, J. K., and Doudna, J. A. (2016) Biology and applications of CRISPR systems: harnessing nature's toolbox for genome engineering. *Cell* **164**, 29–44
4. Cong, L., Ran, F. A., Cox, D., Lin, S. L., Barretto, R., Habib, N., *et al.* (2013) Multiplex genome engineering using CRISPR/Cas systems. *Science* **339**, 819–823
5. Jinek, M., Chylinski, K., Fonfara, I., Hauer, M., Doudna, J. A., and Charpentier, E. (2012) A programmable dual-RNA-guided DNA endonuclease in adaptive bacterial immunity. *Science* **337**, 816–821
6. Mali, P., Yang, L., Esvelt, K. M., Aach, J., Guell, M., DiCarlo, J. E., *et al.* (2013) RNA-guided human genome engineering *via* Cas9. *Science* **339**, 823–826
7. Kanaar, R., Hoeijmakers, J. H., and van Gent, D. C. (1998) Molecular mechanisms of DNA double strand break repair. *Trends Cell Biol.* **8**, 483–489
8. Symington, L. S., and Gautier, J. (2011) Double-strand break end resection and repair pathway choice. *Annu. Rev. Genet.* **45**, 247–271
9. Mao, Z., Bozzella, M., Seluanov, A., and Gorbunova, V. (2008) Comparison of nonhomologous end joining and homologous recombination in human cells. *DNA Repair (Amst)* **7**, 1765–1771
10. Pawelczak, K. S., Gavande, N. S., VanderVere-Carozza, P. S., and Turchi, J. J. (2018) Modulating DNA repair pathways to improve precision genome engineering. *ACS Chem. Biol.* **13**, 389–396
11. Brookhouser, N., Raman, S., Potts, C., and Brafman, D. A. (2017) May i cut in? Gene editing approaches in human induced pluripotent stem cells. *Cells* **6**, 5
12. Rees, H. A., and Liu, D. R. (2018) Base editing: precision chemistry on the genome and transcriptome of living cells. *Nat. Rev. Genet.* **19**, 770–788
13. Huang, T. P., Newby, G. A., and Liu, D. V. R. (2021) Precision genome editing using cytosine and adenine base editors in mammalian cells (vol 16, pg 1089, 2021). *Nat. Protoc.* **16**, 5740
14. Porto, E. M., Komor, A. C., Slaymaker, I. M., and Yeo, G. W. (2020) Base editing: advances and therapeutic opportunities. *Nat. Rev. Drug Discov.* **19**, 839–859
15. Komor, A. C., Kim, Y. B., Packer, M. S., Zuris, J. A., and Liu, D. R. (2016) Programmable editing of a target base in genomic DNA without double-stranded DNA cleavage. *Nature* **533**, 420
16. Gaudelli, N. M., Komor, A. C., Rees, H. A., Packer, M. S., Badran, A. H., Bryson, D. I., *et al.* (2017) Programmable base editing of A*T to G*C in genomic DNA without DNA cleavage. *Nature* **551**, 464–471
17. Lopez-Martinez, D., Kupculak, M., Yang, D., Yoshikawa, Y., Liang, C. C., Wu, R., *et al.* (2019) Phosphorylation of FANCD2 inhibits the FANCD2/FANCI complex and suppresses the fanconi anemia pathway in the absence of DNA damage. *Cell Rep.* **27**, 2990–3005.e5
18. Chang, Y. J., Xu, C. L., Cui, X., Bassuk, A. G., Mahajan, V. B., Tsai, Y. T., *et al.* (2019) CRISPR base editing in induced pluripotent stem cells. *Methods Mol. Biol.* **2045**, 337–346
19. Huang, L., Dong, H., Zheng, J., Wang, B., and Pan, L. (2019) Highly efficient single base editing in Aspergillus Niger with CRISPR/Cas9 cytidine deaminase fusion. *Microbiol. Res.* **223-225**, 44–50
20. Hua, K., Tao, X., Han, P., Wang, R., and Zhu, J. K. (2019) Genome engineering in rice using Cas9 variants that recognize NG PAM sequences. *Mol. Plant* **12**, 1003–1014
21. Zhang, M., Zhou, C., Wei, Y., Xu, C., Pan, H., Ying, W., *et al.* (2019) Human cleaving embryos enable robust homozygotic nucleotide substitutions by base editors. *Genome Biol.* **20**, 101
22. Germini, D., Tsfasman, T., Zakharova, V. V., Sjakste, N., Lipinski, M., and Vassetzky, Y. (2018) A comparison of techniques to evaluate the effectiveness of genome editing. *Trends Biotechnol.* **36**, 147–159
23. O'Geen, H., Ren, C., Nicolet, C. M., Perez, A. A., Halmai, J., Le, V. M., *et al.* (2017) dCas9-based epigenome editing suggests acquisition of histone methylation is not sufficient for target gene repression. *Nucl. Acids Res.* **45**, 9901–9916
24. Ren, C., Xu, K., Segal, D. J., and Zhang, Z. (2019) Strategies for the enrichment and selection of genetically modified cells. *Trends Biotechnol.* **37**, 56–71
25. Zafra, M. P., Schatoff, E. M., Katti, A., Foronda, M., Breinig, M., Schweitzer, A. Y., *et al.* (2018) Optimized base editors enable efficient editing in cells, organoids and mice. *Nat. Biotechnol.* **36**, 888–893
26. Brookhouser, N., Nguyen, T., Tekel, S. J., Standage-Beier, K., Wang, X., and Brafman, D. A. (2020) A Cas9-mediated adenosine transient reporter enables enrichment of ABE-targeted cells. *BMC Biol.* **18**, 193
27. Standage-Beier, K., Tekel, S. J., Brookhouser, N., Schwarz, G., Nguyen, T., Wang, X., *et al.* (2020) A transient reporter for editing enrichment (TREE) in human cells. *Nucl. Acids Res.* **48**, 1602
28. Zuo, E., Sun, Y., Yuan, T., He, B., Zhou, C., Ying, W., *et al.* (2020) A rationally engineered cytosine base editor retains high on-target activity while reducing both DNA and RNA off-target effects. *Nat. Methods* **17**, 600–604
29. Wang, X., Li, J., Wang, Y., Yang, B., Wei, J., Wu, J., *et al.* (2018) Efficient base editing in methylated regions with a human APOBEC3A-Cas9 fusion. *Nat. Biotechnol.* **36**, 946–949
30. Zhou, C., Sun, Y., Yan, R., Liu, Y., Zuo, E., Gu, C., *et al.* (2019) Off-target RNA mutation induced by DNA base editing and its elimination by mutagenesis. *Nature* **571**, 275–278
31. Landrum, M. J., Lee, J. M., Benson, M., Brown, G., Chao, C., Chitipiralla, S., *et al.* (2016) ClinVar: public archive of interpretations of clinically relevant variants. *Nucl. Acids Res.* **44**, D862–868
32. Sun, H., and Yu, G. (2019) New insights into the pathogenicity of non-synonymous variants through multi-level analysis. *Sci. Rep.* **9**, 1667
33. Brookhouser, N., Tekel, S. J., Standage-Beier, K., Nguyen, T., Schwarz, G., Wang, X., *et al.* (2020) BIG-TREE: Base-Edited isogenic hPSC line generation using a transient reporter for editing enrichment. *Stem Cell Rep.* **14**, 184–191
34. Katti, A., Foronda, M., Zimmerman, J., Diaz, B., Zafra, M. P., Goswami, S., *et al.* (2020) GO: a functional reporter system to identify and enrich base editing activity. *Nucl. Acids Res.* **48**, 2841–2852
35. Wang, P., Xu, L., Gao, Y., and Han, R. (2020) BEON: a functional fluorescence reporter for quantification and enrichment of adenine base-editing activity. *Mol. Ther.* **28**, 1696–1705

ASBMB

36. Coelho, M. A., Li, S., Pane, L. S., Firth, M., Ciotta, G., Wrigley, J. D., *et al.* (2018) BE-FLARE: a fluorescent reporter of base editing activity reveals editing characteristics of APOBEC3A and APOBEC3B. *BMC Biol.* **16**, 150
37. Martin, A. S., Salamango, D. J., Serebrenik, A. A., Shaban, N. M., Brown, W. L., and Harris, R. S. (2019) A panel of eGFP reporters for single base editing by APOBEC-Cas9 editosome complexes. *Sci. Rep.* **9**, 497
38. Tekel, S. J., Brookhouser, N., Standage-Beier, K., Wang, X., and Brafman, D. A. (2021) Cytosine and adenosine base editing in human pluripotent stem cells using transient reporters for editing enrichment. *Nat. Protoc.* **16**, 3596–3624
39. Ran, F. A., Hsu, P. D., Wright, J., Agarwala, V., Scott, D. A., and Zhang, F. (2013) Genome engineering using the CRISPR-Cas9 system. *Nat. Protoc.* **8**, 2281–2308
40. Mansour, W. Y., Rhein, T., and Dahm-Daphi, J. (2010) The alternative end-joining pathway for repair of DNA double-strand breaks requires PARP1 but is not dependent upon microhomologies. *Nucl. Acids Res.* **38**, 6065–6077
41. Ren, C., Xu, K., Liu, Z., Shen, J., Han, F., Chen, Z., *et al.* (2015) Dual-reporter surrogate systems for efficient enrichment of genetically modified cells. *Cell Mol. Life Sci.* **72**, 2763–2772
42. Yan, N., Sun, Y., Fang, Y., Deng, J., Mu, L., Xu, K., *et al.* (2020) A universal surrogate reporter for efficient enrichment of CRISPR/Cas9-Mediated homology-directed repair in mammalian cells. *Mol. Ther. Nucl. Acids* **19**, 775–789
43. Joung, J., Konermann, S., Gootenberg, J. S., Abudayyeh, O. O., Platt, R. J., Brigham, M. D., *et al.* (2017) Genome-scale CRISPR-Cas9 knockout and transcriptional activation screening. *Nat. Protoc.* **12**, 828–863
44. Hanna, R. E., Hegde, M., Fagre, C. R., DeWeirdt, P. C., Sangree, A. K., Szegletes, Z., *et al.* (2021) Massively parallel assessment of human variants with base editor screens. *Cell* **184**, 1064–1080.e20
45. Cuella-Martin, R., Hayward, S. B., Fan, X., Chen, X., Huang, J. W., Taglialatela, A., *et al.* (2021) Functional interrogation of DNA damage response variants with base editing screens. *Cell* **184**, 1081–1097.e19
46. Chen, R., Greene, E. L., Collinsworth, G., Grewal, J. S., Houghton, O., Zeng, H., *et al.* (1999) Enrichment of transiently transfected mesangial cells by cell sorting after cotransfection with GFP. *Am. J. Physiol.* **276**, F777–F785
47. Zhang, X., Zhu, B., Chen, L., Xie, L., Yu, W., Wang, Y., *et al.* (2020) Dual base editor catalyzes both cytosine and adenine base conversions in human cells. *Nat. Biotechnol.* **38**, 856–860
48. Xu, L., Liu, Y., and Han, R. J. T. C. J. (2019) BEAT: a Python program to quantify base editing from sanger sequencing. *CRISPR J.* **2**, 223–229